ADVANCED MATERIALS
www.advmat.de

A New Conducting Polymer with Exceptional Visible-Light Photocatalytic Activity Derived from Barbituric Acid Polycondensation

Neda Keshavarzi, Shaowen Cao, and Markus Antonietti*

A novel covalent, metal-free, photocatalytic material is prepared by thermal polymerization of barbituric acid (BA). The structure of the photocatalyst is analyzed by using scanning electron microscopy, X-ray diffraction, and infrared, UV–visible, and ^{1}H solution and ^{13}C solid-state NMR spectroscopy. The photodegradation efficiency of BA thermally polymerized at different temperatures is tested by photocatalytic degradation of aquatic rhodamine B (RhB) dye under visible-light irradiation. It is shown that heating BA at an optimized temperature of 300 °C, that is, still in the range that polymer-like polycondensation takes place, results in a photocatalyst that can remove RhB with 96% photodegradation efficiency after 70 min exposure to visible light. The polycondensation reaction of BA is identified to process through precipitation of trimer units as primary building blocks. Reference experiments such as addition of scavengers and saturation with oxygen are studied to understand the photodegradation process. It is shown that the presence of triethanolamine, and excess of oxygen and p-benzoquinone in the solution of RhB and photocatalyst (BA300) is not beneficial, but decreases the photodegradation efficiency.

Barbituric acid (BA) is a simple and omnipresent organic molecule, which just recently is employed as a comonomer for designing new carbon nitride materials.[1] Copolymerization is extensively used to tune the structure of g-C_3N_4 and subsequently to improve the photocatalytic performance. Previous studies showed that adding BA in a system containing melamine and cyanuric acid improves the optical density of final covalent semiconductor material.[2,3] This enhancement is due to the extension of optical absorption to the visible range as a direct result of copolymerization with BA.[4] Despite of large amount of research on the use of BA in supramolecular chemistry, there is a little known about its use as a monomer for condensation as such, that is, the structural changes and characteristic properties of BA as a single monomer to generate a semiconducting polymer. It is known that the methylene group ($-CH_2$) in BA is an active group and can react in condensation reactions with other monomers.[5] Moreover the carbon at the C-5 position in the BA molecule can also form noncovalent hydrogen bonds with other complementary monomers to prealign and form functional materials.[6] In this work, we present the thermal polycondensation of BA, which proceeds rather well controlled and gives first a crystalline trimer, then a functional, polymer semiconductor. The physical properties, chemical composition, microstructure, morphology, and optical properties of these polymer resins condensed at different temperatures are analyzed by thermogravimetric analysis (TGA), CHNO elemental analysis, scanning electron microscopy (SEM), N_2 adsorption–desorption analysis, Fourier transform infrared (FT-IR) spectroscopy, X-ray diffraction, solution and solid-state nuclear magnetic resonance NMR, and UV–visible spectroscopy. Furthermore, the photocatalytic performance of this organic semiconductor is exemplified by the efficient photodegradation of rhodamine B (RhB) under visible-light illumination. RhB is a cationic dye and an aquatic pollutant released by textile, plastic, and dye industries, but here only taken as a robust model compound.[7,8]

TGA is commonly used to study the onset of thermal condensation reactions and the ultimate thermal stability of polymeric materials.[9] TGA of BA shows stepwise weight loss with three sharp steps speaking for distinct, well-defined elimination/condensation reactions. In addition, a final total mass loss of 95% at 900 °C is observed, indicating that the condensed material is not carbonaceous (**Figure 1**a). BA releases a small amount, 0.4% by mass, of loosely bound surface adsorbed moisture starting at 35 °C. The first significant mass loss by 66% is sharply proceeding between 238 and 296 °C due to the combination of water loss as a result of condensation reactions and partial sublimation. The as formed polymer is obviously rather stable up to 400 °C, until a second mass loss with an onset at 410 °C corresponding to 13% initial mass loss occurs. We will relate that step down below to slower, secondary

Dr. N. Keshavarzi, Prof. M. Antonietti
Max Planck Institute of Colloids and Interfaces
Am Mühlenberg 1, 14476 Potsdam, Germany
E-mail: Neda.Keshavarzi@mpikg.mpg.de
Dr. S. Cao
State Key Lab of Advanced Technology Materials Synthesis & Processing
Wuhan University of Technology
Wuhan 430070, Hubei, P. R. China
The ORCID identification number(s) for the author(s) of this article can be found under https://doi.org/10.1002/adma.201907702.

DOI: 10.1002/adma.201907702

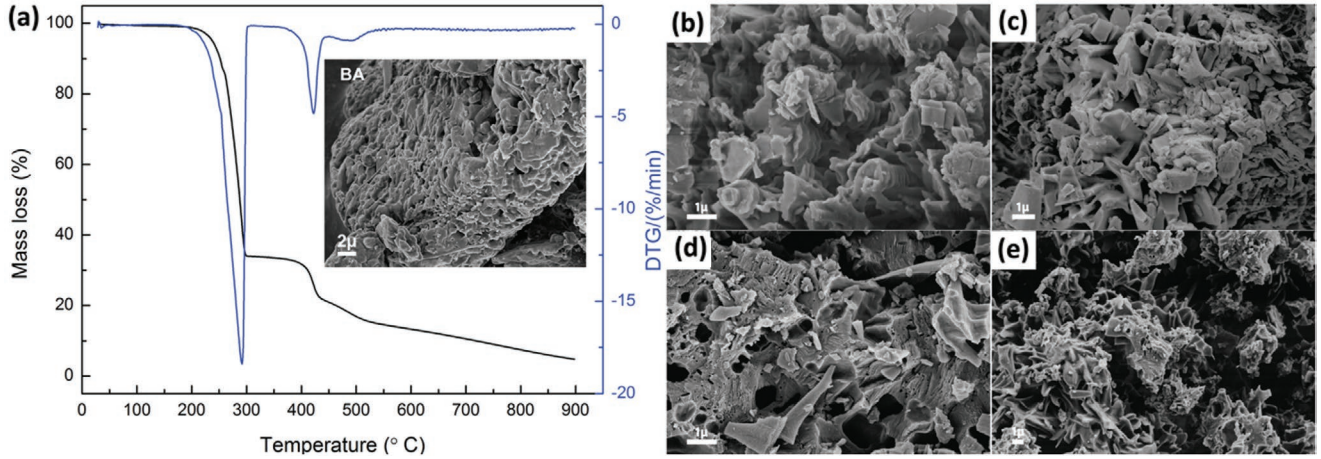

Figure 1. a) Thermogravimetric analysis of barbituric acid (BA) under the flow of N_2 gas and inset presenting SEM microstructure of as-received BA powder. b–e) SEM pictures of BA thermally condensed with heating rate of 20 °C min^{-1} for 4 h in nitrogen atmosphere at 300 °C (b), 350 °C (c), 450 °C (d), 550 °C (e).

condensation reactions forming a 3D material. A third peak slightly below 500 °C marks the final onset of less controlled carbonization of the sample. The thermal events at 291, 422, and 488 °C can be seen as sharp and pronounced peaks observed on the derivative curve in Figure 1a. Using SEM, we find that the microstructure at 300 °C (BA300, Figure 1b), resembles a morphology close to BA powder (Figure 1a inset) but with distinct cavities in an otherwise mostly prevailed structure, that is, the mass loss is mostly related to a condensation of the monomer, either in a topotactic fashion or by a melting–reprecipitation process[9] The particles flatten and thin out by heating to 350 °C (BA350, Figure 1c), while a porous, irregular structure evolves as BA is further heated up to 450 °C (BA450, Figure 1d) and 550 °C (BA550, Figure 1e). As indicated by TGA, this marks the transition from monomer to well defined condensates to finally polymer-based carbon materials. The surface area usually has an important role in heterogeneous photocatalysts.[10] Nitrogen adsorption analysis in **Figure 2** and porosity analysis in Table S1, Supporting Information confirms TGA and SEM findings. BA heated at 300 and 350 °C has a low specific surface area of 6 and 2 m^2 g^{-1}, obtained from the *t*-plot which goes well with the outer surface of the particles observed by SEM. Furthermore, the type of N_2 adsorption–desorption isotherms confirm the existence of slit-shaped pores formed by plate-like particles.[11] Surface area only slightly increases with further condensation above 350 °C, thus excluding the formation of a pronounced inner pore system at higher temperatures. Analysis of elemental composition in **Table 1** shows that under nitrogen flow, up to 350 °C the nitrogen and carbon content increases under preservation of the C/N ratio while hydrogen and oxygen contents decreases. A C/N = 1.9 observed after simple heating at 350 °C is indeed very close to the original C/N = 2 of BA and the small difference is within experimental uncertainties, thus supporting that water elimination is the dominant reaction. For illustration, we might give the following idealized reaction condensation step, going with the specific relative reactivities of BA, as shown in **Scheme 1**.

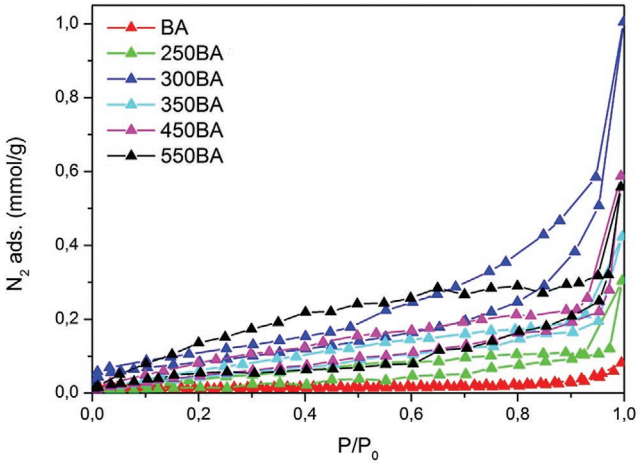

Figure 2. Nitrogen adsorption analysis of as received barbituric acid powder and barbituric acid condensed at temperatures between 250 and 550 °C with heating rate of 20 °C min^{-1} for 4 h in nitrogen atmosphere.

In spite of the less defined thermal condensation at higher temperatures, the increase of N and C goes on up to 550 °C, with only slight loss of N, but mostly oxygen, presumably as water. It is clear that the presented idealized primary linear oligomer structure can undergo further 3D condensation and aromatization, with the OH groups being the condensation

Table 1. CHNO elemental analysis of the barbituric acid before and after condensation at temperatures between 250 and 550 °C for 4 h under flow of nitrogen.

Material	N [%]	C [%]	H [%]	O [%]	C/N molar ratio	Empirical formula
Barbituric acid (BA)	20.4	37.7	3.29	36.3	2.15	$C_{4.1}H_{4.3}N_{1.9}O_3$
BA, 250 °C	21.3	37.7	3.03	36.1	2.06	$C_{4.1}H_4N_2O_3$
BA, 300 °C	24.0	40.0	3.01	30.6	1.94	$C_{4.4}H_{3.9}N_{2.2}O_{2.5}$
BA, 350 °C	24.8	40.6	3.00	29.4	1.90	$C_{4.5}H_{3.9}N_{2.3}O_{2.4}$
BA, 450 °C	29.3	55.4	2.65	13.6	2.20	$C_{6.1}H_{3.5}N_{2.7}O_{1.1}$
BA, 550 °C	28.8	58.9	2.23	10.2	2.38	$C_{6.5}H_{2.9}N_{2.7}O_{08}$

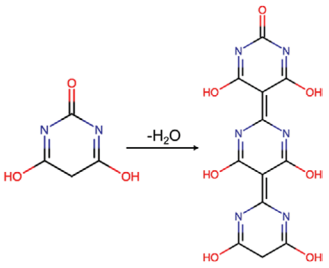

Scheme 1. Idealized illustration of barbituric acid thermal condensation reaction by water elimination forming crystalline trimer.

points. The observed C/N molar ratios (Table 1) also confirms that we are far from the otherwise rather structure-determining C_3N_4 formation, that is, the BA condensation clearly follows a different, new thermodynamic path. Structural changes in BA thermally treated at different temperatures can be characterized by X-ray diffraction. **Figure 3**a show that low-angle peaks at 2θ = 6.94°, 9.94°, and 13.6° appear when BA is heated to 300 and 350 °C, clearly indicating the mesoscale organization of a new oligomeric species, most probably driven by excessive hydrogen bridges of OH and N. Peaks at 13.6° and 27.8° are related to (100) and (002) crystallographic planes indicating presence of aromatic stacking of conjugated systems (002) and in-planar repetition of aromatic units (100) similar to those observed in graphitic carbon nitride materials but also in other conducting polymers.[12,13] The peak at 27.8° becomes broader and shifts to lower angles at higher temperatures, thus proving that secondary lateral condensation induces disorder in local packing. The peak appearance at lower angles shows that a structure with a well-defined order is formed at 300 °C, different to the primary BA, but rather too-well crystalline for a polymer, which is in agreement with the SEM morphologies in Figure 1b. The peaks diminish (but stay in position) by further heating at 350 °C (Figure 3a), pointing to different extents of polymerization. The infrared signal of BA heated at 300 and 350 °C (Figure 3b) follows the structural changes observed by X-ray diffraction.[14] Strong stretching vibration of carbonyl group (C=O) is broadened and shifted from 1682 to 1571 cm^{-1} due to formation of new C—C bonds. The peaks at the lower end of the spectra at 626, 689, and 825 cm^{-1} are related to ring puckering and C—H bending vibrations, which are broadened when BA is heated at 300 and 350 °C.[15,16] Both X-ray and infrared data shows that heating beyond 350 °C results in a carbonaceous material with less structural definition. A comparison of ^{1}H NMR spectra of BA before and after thermal condensation at 300 °C (BA300) helps to resolve the structures involved in the condensation reaction and is presented in **Figure 4**a.[17] It is clear that the potentially oligomeric product is very well defined in structure, but has completely changed. The peaks suggest a structure composed of electron-poor aromatic units plus some very acidic protons at high chemical shifts after condensation. The signal related to acidic proton of N—H bond at δ = 11.113 ppm in BA is considerably reduced after condensation due to formation of a new conjugated system with different proton affinity, and indeed, we find no leftovers of the former BA motif. Furthermore, the signal at δ = 3.463 ppm, which is related to protons attached to sp^2 carbon (C—H), shifts to higher values, but stay strong, pointing to the significant existence of a related, but new terminal group at 300 °C. The ratio of the integrated C—H signal of BA to BA300 is 0.247, which is very close to the trimer shown in Scheme 1 (BA/trimer: 0.25), which obviously has precipitated from the reaction mixture as the primary product of condensation reaction. In Figure 4b, solid-state ^{13}C NMR spectra of BA before and after thermal condensation at 300 °C (BA300) and 350 °C (BA350) are shown for comparison. Primary carbon signals of C—H at δ = 40 ppm in BA completely disappear after condensation at 300 and 350 °C. This is again confirming that sp^2 carbon (C–H) are significantly involved in the condensation reactions. However, new peaks appear at δ = 84, 85, and 90 ppm due to new carbon bonds in the structure, that is, C=C. The signal at δ = 151 ppm attributed to the carbonyl group (C=O) connected to two N atoms in BA splits into three peaks but remains at the same position after condensation at 300 and 350 °C. The carbonyl groups connected to sp^2 carbon appear at δ = 170 ppm in BA but split into three peaks and shift to slightly lower chemical shift values after condensation at 300 °C and 350 °C. Signal splitting in BA after condensation reflects

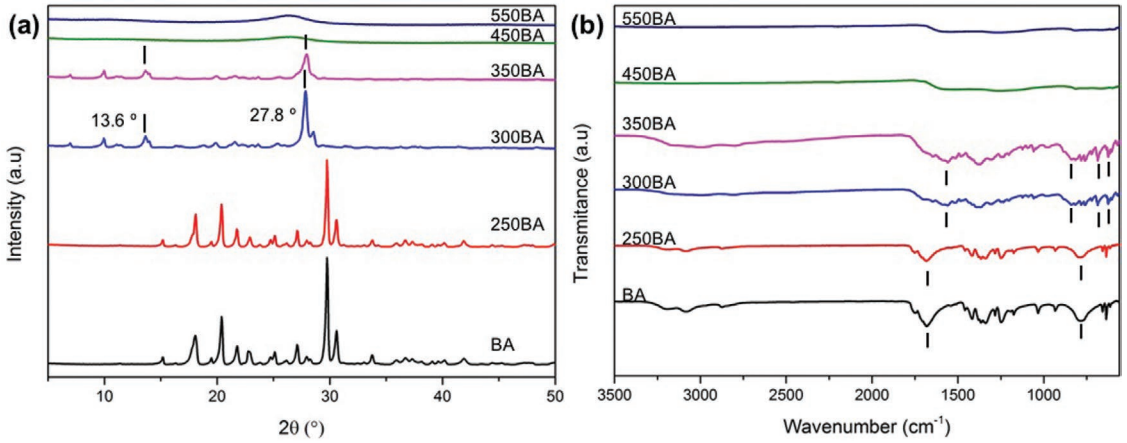

Figure 3. a) X-ray diffraction pattern and b) infrared spectra of barbituric acid before and after condensation at temperatures between 250 and 550 °C for 4 h under flow of nitrogen.

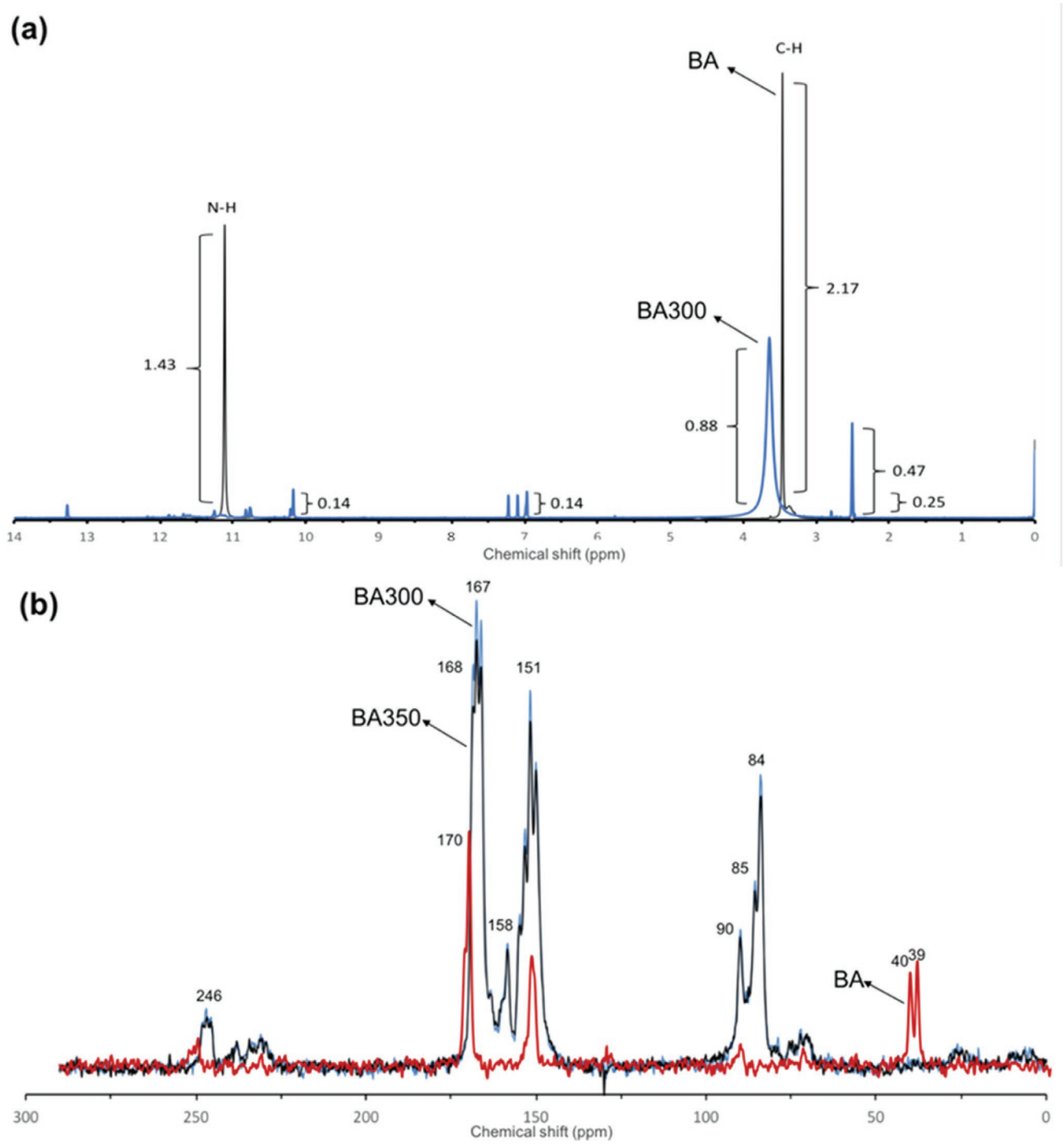

Figure 4. a) ^{1}H solution NMR spectra with DMSO as reference and the integrated peak intensities of barbituric acid (BA) before and after thermal condensation at 300 °C (BA300) for 4 h under flow of nitrogen. The integrated intensities are given alongside of the brackets. b) ^{13}C solid-state NMR spectra for BA before and after condensation at 300 and 350 °C (BA300 and BA350) for 4 h under flow of nitrogen. Numbers on top of peaks present respective chemical shift of each peak in ppm.

the enlarged delocalization of the conjugated electronic system in the new structure.[18]

BAs condensed at different temperature have different colors as is shown in **Figure 5**a. BAs condensed at 300 and 350 °C have promising optical properties, going well with a conducting, medium-bandgap polymer semiconductor. The development and redshift in the absorption band edge of thermally condensed BAs observed in the UV–vis spectra in Figure 5b correspond to the formation of a new oligomeric, crystalline semiconductor material at 300–350 °C, with the probability that BA condensed at 350 °C is already slightly polymerized. BAs thermally condensed at 300 and 350 °C show improved optical absorption intensity

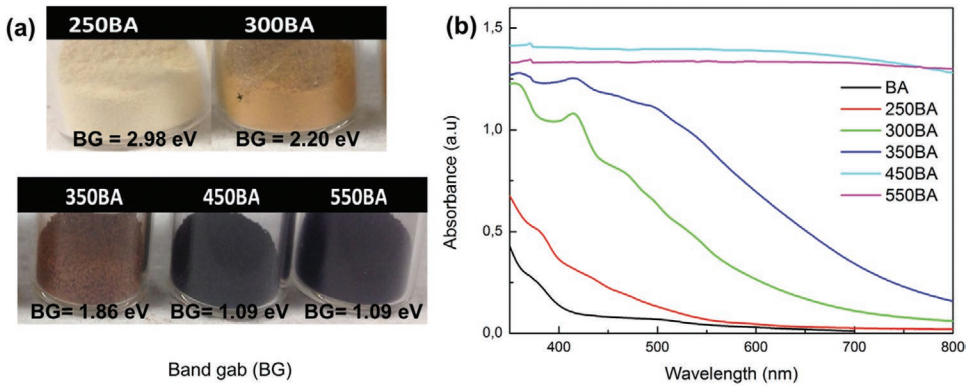

Figure 5. a) Optical images with the respective bangaps and b) UV–vis spectra of barbituric acid after condensation at temperatures between 250 and 550 °C for 4 h under flow of nitrogen.

extended to higher visible range with a bandgap of 2.20 and 1.86 eV, respectively. The absorption tail is raised and extended to longer wavelength up to 900 nm by increasing the temperature at which BA is condensed, due to the formation of defects and the highly conjugated system.[19] BAs condensed at 450 °C and 500 °C show a black color, demonstrated by the absorbance spectra. Therefore, condensation at higher temperatures above 350 °C narrows the bandgap and makes BA more "carbon-like". The photoactivity of the thermally condensed BA is evaluated by measuring the RhB degradation rate by exposure to visible-light illumination. The degradation rate is estimated using the linear relationship between $\ln\left(\frac{C}{C_0}\right)$ and irradiation time according to the first-order Equation (1):

$$-\ln\left(\frac{C}{C_0}\right) = kt \tag{1}$$

where k is the slope of line that represents the relationship between the natural logarithm of the initial RhB concentration (C_0) and the RhB concentration after light illumination (C), as a function of irradiation time (t). Here, k is the rate constant and indicates the photocatalytic activity of the condensed BA. The photodegradation efficiency is obtained from the following formula in Equation (2):

$$\text{Degradation efficiency} = \frac{c - c_0}{c_0} \times 100 \tag{2}$$

Rate constants calculated from the UV–vis spectra show that RhB degrades three times faster in the presence of the 300 °C sample (**Figure 6**a,b, K_{300} = 0.029 min^{-1} vs K_{350} = 0.007 min^{-1}). It can be seen that after 70 min of visible light exposure in the presence of BA condensed at 300 °C, the RhB photodegradation efficiency is 96%. Degradation by the 350 °C sample is less, as a strong signal after 70 min illumination (Figure 6b) represents only 43% photodegradation efficiency. The photodegradation test proves that BA condensed at 300 °C to the oligomer crystal has an optimum conjugated electronic system and is a semiconductor with a bandgap of 2.20 eV and beneficial charge conduction and localization at outer surfaces. To learn more about the photoreaction mechanism, we performed certain reference experiments. Oxygen (O_2) is a known key factor in photoreduction process mediated by photogenerated electrons that helps to produce hydroxyl (OH^-) and superoxide (O_2^-) free radicals. The effect of O_2 on photodegradation of RhB is studied by illuminating light to a dispersion of the 300 °C samples mixed with RhB prepared under two conditions: the first dispersion saturated with oxygen and the second dispersion was deaired by vacuum and purged with argon. The degradation rate of RhB interestingly decreased significantly when dispersion is saturated with O_2 as can be seen in Figure 6c, however, deairing did not have an effect on photodegradation rate. This proves that photodegradation does not process via the photoreduction of oxygen. Previous studies on carbon nitrides showed that photodegradation of RhB happens in this case through the photogenerated holes.[19] Experiments with addition of electron scavengers such as silver nitrate ($AgNO_3$) and hole scavengers including methanol and triethanolamine (TEOA) are conducted.[20,21] The results show that $AgNO_3$ and methanol do not affect RhB photodegradation rate in the presence of BA300. However, as shown in Figure 6d, addition of TEOA (5 vol%) significantly decreases the photodegradation rate after 60 min by a factor of 7,that is, we find a photodegradation efficiency of 17% after 70 min exposure to visible light in the presence of TEOA. These data indicate that the RhB degradation is going through photogenerated holes on the valance band of thermally condensed BA, and that TEOA is an effective hole scavenger that interrupts with this process. The photobleaching is thereby a direct photooxidation of the dye. Further experiments are performed using isopropyl alcohol (IPA) (0.02 M) and *p*-benzoquinone (BZQ, 0.001 M) as scavengers for hydroxyl radicals (•OH) and superoxide anion radicals ($\bullet O_2^-$), respectively. Figure S1, Supporting Information shows that IPA does not affect RhB photodegradation rate in the presence of BA300. On the other hand, the addition of BZQ significantly decreases the photodegradation rate to a photodegradation efficiency of 23% after 80 min. These results suggest that the RhB degradation is also going through superoxide anion radicals. The adsorption properties toward RhB of all the as-prepared samples are shown in Figure S2, Supporting Information. The RhB adsorption efficiency is 10%, 12%, and 6% for BA250, BA300, and BA350 after 90 min, and is negligible for BA450 and BA500.The RhB adsorption efficiency of BA300 is twice of BA350 due to presence of higher numbers of OH groups on BA300 surface.

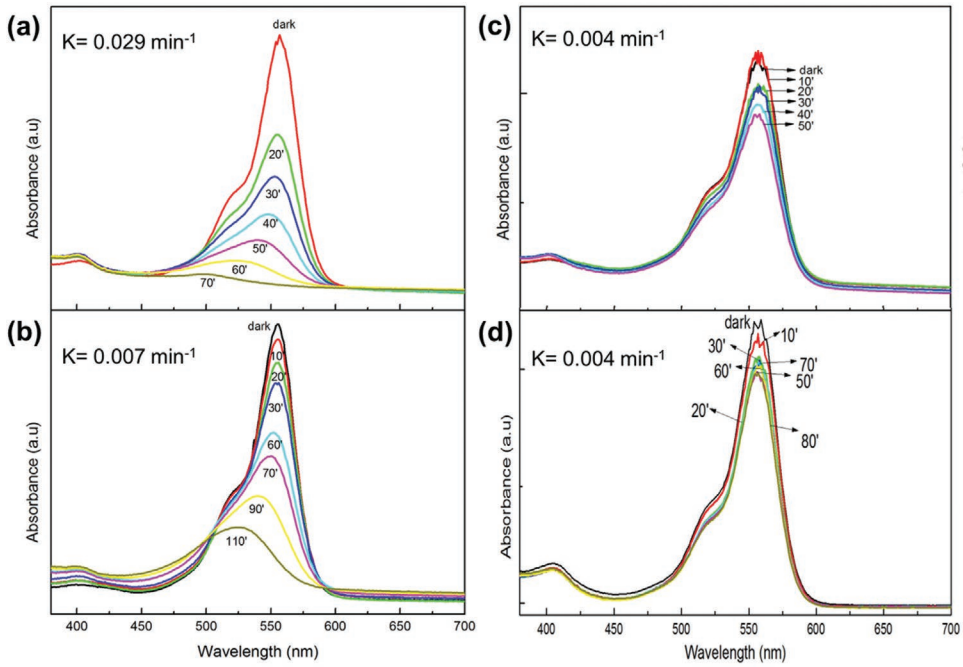

Figure 6. a–d) UV–vis absorption spectra representing photodegradation of rhodamine B (RhB) as a function of illumination time in: a) BA300 solution; b) BA350 solution; c) BA300 solution saturated with O_2, and d) BA300 solution containing tetraethanolamine. The dark spectrum represents the light absorption of RhB and thermally condensed barbituric acid (BA-condensation temperature) solution stirred in the dark for 30 min before light illumination.

In summary, BA was condensed by simple and reproducible thermal treatment to form semiconductor oligomeric materials with a well-defined structure. Thermal treatment temperature was optimized, and BAs condensed at 300 and 350 °C with a bandgap of 2.20 and 1.86 eV demonstrated excellent visible-light absorption due to presence of highly polarizable conjugated system in the structure. The structure of condensed BA was identified to be a trimer as the primary product of condensation reaction, which crystallizes and precipitates from the reaction mixture. Our results confirm that BA condensed at 300 °C shows exceptionally high photocatalytic activities, three times higher than BA condensed at 350 °C, under visible-light illumination and is able to remove RhB dye from water solution with 96% photodegradation efficiency. The photocatalytic RhB degradation is directly related to the photogenerated holes on the valance band of thermally condensed BA showing that photobleaching is thereby a direct photooxidation of dye. In good agreement with this scheme, the presence of a strong hole scavenger interrupts the reaction significantly. Our conductive oligomeric structure shows significant potential as a novel efficient photocatalyst for applications in pollution elimination or possibly for hydrogen evolution or photoelectric current generation using visible range solar radiation.

Experimental Section

Materials and Methods: Barbituric acid (BA, 99%, Alfa Aesar, GmbH & Co. KG) was used as the starting monomer for polycondensation reaction. RhB (dye content 95%, Sigma-Aldrich, Gmbh) was used as the target dye in photodegradation. For polycondensation reaction BA (0.5 g) was placed in alumina crucible and heated in an oven for 4 h with heating rate of 20 °C min^{-1} at 250 °C (BA250), 300 °C (BA300), 350 °C (BA350), 450 °C (BA450), and 550 °C (BA550). For photodegradation test RhB solution (M = 20 ppm) was prepared by dissolving RhB powder (2 mg) into distilled water (100 mL). The photodegradation of RhB was performed by dispersing condensed BA (5 mg) in RhB solution (20 mL, 20 ppm) then leaving the dispersion in dark for 30 min under stirring prior to light illumination. Reference experiments were performed using electron–hole scavengers including silver nitrate (1 mL, 0.1 M $AgNO_3$, Sigma-Aldrich, Gmbh), methanol (1 mL, Merck), and triethanolamine (1 mL, TEOA 98%, Alfa Aesar GmbH). IPA (0.02 M, ≥99.7%, Sinopharm Chemical Reagent Co., Ltd.) and p-benzoquinone (0.001 M, ≥99.7%, Sinopharm Chemical Reagent Co., Ltd.) were employed as scavengers for hydroxyl radicals (•OH) and superoxide anion radicals ($\bullet O_2^-$), respectively. To study the effect of oxygen the RhB-catalyst solutions were prepared in two ways. First, solution of catalyst and RhB was deaired by stirring under vacuum overnight and then purged with argon for 30 min to remove all oxygen. Second, dispersion of RhB and catalyst was prepared by purging solution with oxygen for 30 min to obtain an oxygen saturated solution. In all these tests the RhB-catalyst solution was stirred in dark for 30 min before illumination with light in order to obtain an adsorption–desorption equilibrium between RhB and catalyst particles. The adsorption efficiency of RhB on condensed BA was then measured using UV–vis spectra. The UV–vis spectra of 30 min stirred solution before illumination was the so-called dark spectrum.

Characterization: X-ray diffraction patterns as measured on a Bruker D8 Advance instrument using Cu-Kα-radiation. Infrared spectra of the material were collected using iS5 FT-IR spectrometer with Thermo Scientific iD5 Diamond ATR. The adsorption and desorption isotherms of N_2 at 77 K was measured on samples after degassing at 150 °C under vacuum for 20 h using a Quantachrome Quadrasorb SI porosimeter. The surface area was calculated by applying Brunauer–Emmett–Teller

model to the adsorption branch between 0.05 and 0.15 P/P_0. CHNO analysis is conducted by combustion analysis using a Vario Micro device at 1150 °C in helium atmosphere. SEM images were obtained on a LEO 1550-Gemini at an accelerating voltage of 3 KV. Samples were coated with 5–10 nm layer composed of 80% gold and 20% palladium prior to SEM examination to avoid charge up effect. Solution NMR spectroscopy was performed on A Bruker AVANCE 700 MHz Nuclear Magnetic Resonance Spectrometer equipped with a 5 mm cryoprobe and a Z-axis pulse field gradient was used throughout this study. The key acquisition parameters for ^{1}H NMR spectra was 512 scans, spectral width 6410.25 Hz with 32 768 acquired datapoints with DMSO as standard reference. Magic-angle solid-state NMR spectroscopy was performed on a Bruker AVANCE 900 MHz Nuclear Magneti with 2048 acquired datapoints. LED white light ($\lambda > 410$ nm, 100 W, X2Labware Singapore) was used as a light source to illuminate solution containing RhB and catalyst for the photodegradation experiment. Degradation of RhB was analyzed by measuring the remaining amount of RhB in solution at different time intervals by UV–vis absorption spectra using Varian Cary 50 UV–VIS spectrometer. Optical absorption spectra of powder samples were recorded using SHIMADZU UV-2600.

Supporting Information

Supporting Information is available from the Wiley Online Library or from the author.

Acknowledgements

The authors would like to thank Max Planck Institute of Colloids and Interfaces, especially Prof. Markus Antonietti for providing the research funding for this project and his significant scientific input in manuscript preparation.

Conflict of Interest

The authors declare no conflict of interest.

Author Contributions

N.K. contributed to planning and performing the experiments, data analysis, and writing of the manuscript. S.C. contributed with performing important experiments presented as supporting information.

Keywords

barbituric acid, conducting polymers, photocatalysts, rhodamine B, visible-light photocatalytic activity

Received: November 23, 2019
Revised: January 22, 2020
Published online:

[1] Y. Zheng, L. Lin, B. Wang, X. Wang, *Angew. Chem., Int. Ed.* **2015**, *54*, 12868.
[2] Y. S. Jun, E. Z. Lee, X. Wang, W. H. Hong, G. D. Stucky, A. Thomas, *Adv. Funct. Mater.* **2013**, *23*, 3661.
[3] M. Shalom, M. Guttentag, C. Fettkenhauer, S. Inal, D. Neher, A. Llobet, M. Antonietti, *Chem. Mater.* **2014**, *26*, 5812.
[4] J. Zhang, X. Chen, K. Takanabe, K. Maeda, K. Domen, J. D. Epping, X. Fu, M. Antonietti, X. Wang, *Angew. Chem., Int. Ed.* **2009**, *49*, 441.
[5] B. S. Jursic, *J. Heterocycl. Chem.* **2001**, *38*, 655.
[6] B. J. Cafferty, D. M. Fialho, J. Khanam, R. Krishnamurthy, N. V. Hud, *Nat. Commun.* **2016**, *7*, 11328.
[7] M. Hassanpour, H. S. Hojaghan, M. S. Niasari, *J. Mol. Liq.* **2016**, *229*, 293.
[8] J. J. Zhang, S. S. Fang, J. Y. Mei, G. P. Zheng, X. C. Zheng, X. X. Guan, *Sep. Purif. Technol.* **2017**, *194*, 96.
[9] X. Cao, Y. Li, B. Liu, A. Gao, J. Cao, Y. Yu, X. Hei. *New J. Chem.* **2019**, *43*, 7093.
[10] C. Yang, W. Dong, G. Cui, Y. Zhao, X. Shi, X. Xia, B. Tang, W. Wang. *Sci. Rep.* **2017**, *7*, 3973.
[11] K. S. W. Sing, *Pure Appl. Chem.* **1985**, *57*, 603.
[12] S. Yang, Y. Gong, J. Zhang, L. Zhan, L. Ma, Z. Fang, R. Vajtai, X. Wang, P. M. Ajayan, *Adv. Mater.* **2013**, *25*, 2452.
[13] X. Huang, Z. Wu, H. Zheng, W. Dong, W. Wang. *Green Chem.* **2018**, *20*, 664.
[14] C. Zhou, C. Lai, D. Huang, G. Zeng, C. Zhang, M. Cheng, L. Hu, J. Wan, W. Xiong, M. Wen, L. Qin. *Appl. Catal., B.* **2018**, *220*, 202.
[15] J. Liu, T. Zhang, Z. Wang, G. Dawson, W. Chen, *J. Mater. Chem.* **2011**, *21*, 14398.
[16] Y. Ishida, L. Chabanne, M. Antonietti, M. Shalom, *Langmuir* **2014**, *30*, 447.
[17] S. Elavarasan, B. Baskar, C. Senthil, P. Bhanja, A. Bhaumik, P. Selvam, M. Sasidharan, *RSC Adv.* **2016**, *6*, 49376.
[18] A. Shi, H. Li, S. Yin, B. Liu, J. Zhang, Y. Wang, *Appl. Catal., B.* **2017**, *218*, 137.
[19] S. C. Yan, Z. S. Li, Z. G. Zou, *Langmuir* **2010**, *26*, 3894.
[20] M. Shen, M. A. Henderson, *J. Phys. Chem. Lett.* **2011**, *2*, 2707.
[21] X. Wang, K. Maeda, A. Thomas, K. Takanabe, G. Xin, J. M. Carlsson, K. Domen, M. Antonietti, *Nat. Mater.* **2009**, *8*, 76.